Geoderma 428 (2022) 116206

Contents lists available at ScienceDirect

Geoderma

journal homepage: www.elsevier.com/locate/geoderma

Long-term artificial drainage altered the product stoichiometry of denitrification in alpine peatland soil of Qinghai-Tibet Plateau

Yuechen Tan [a], Yifei Wang [a], Zhu Chen [b], Mengying Yang [c], Yu Ning [a], Chunyan Zheng [d], Zhangliu Du [c], Roland Bol [e,f], Di Wu [c,*]

[a] Institute of Ecological Conservation and Restoration, Chinese Academy of Forestry, Beijing 100091, China
[b] College of Agriculture, Guizhou University, Guiyang 550025, China
[c] Beijing Key Laboratory of Biodiversity and Organic Farming, College of Resources and Environmental Sciences, China Agricultural University, Beijing 100193, China
[d] Hebei Key Laboratory of Soil Ecology, Center for Agricultural Resources Research, Institute of Genetics and Developmental Biology, Chinese Academy of Sciences, Shijiazhuang 050021, China
[e] Institute of Bio- and Geosciences, Agrosphere (IBG-3), Forschungszentrum Jülich GmbH, 52425 Jülich, Germany
[f] School of Natural Sciences, Environment Centre Wales, Bangor University, Bangor, LL57 2UW, UK

ARTICLE INFO

Handling Editor: Daniel Said-Pullicino

Keywords:
Alpine peatland
Rewetting
N deposition
Oxic to anoxic transition
Production source

ABSTRACT

Peatlands, which play a vital role in the global storage of carbon (C) and nitrogen (N), have been artificially drained worldwide over the last few decades. However, the effects of long-term artificial drainage on the soil N cycle and subsequent potent greenhouse gas emissions in peatland soils are not fully understood. In this study, we investigated the effect of drainage on soil properties, aboveground and belowground community compositions, and the N cycle-related functional gene abundances in the world's largest alpine peatland (Zoige Peatland, Qinghai-Tibet Plateau), which has been artificially drained for the past 50 years. We further examined the different responses of soil-borne CO_2, N_2O, and N_2 emissions to three successive "hot moment" events (rewetting, nitrogen deposition, and an oxic-to-anoxic transition) between the drained and natural alpine peatlands using a robotized continuous flow system under an He/O_2 atmosphere. A markedly lower CO_2 flux (34%) was observed in drained peatlands compared to natural peatlands, likely associated with the increased soil bulk density, plant species diversity, and microbial diversity in the former. The N_2O emissions in the drained peatland were 45% lower than those in the natural peatland under oxic conditions, with the ^{15}N-N_2O site-preference (SP) value indicating a higher denitrification contribution in the drained peatland (57%) than in the natural peatland (42%). In contrast, under anoxic conditions, higher N_2O emissions (52%), lower denitrification rates (20%), lower denitrification functional gene abundances (*nirK*: 34%; *nirS*: 19%; *nosZ*: 24%), and lower N_2 emissions (36%) were observed in drained peatlands than in natural alpine peatlands. Molecular analyses further suggested that the different responses of N_2O emissions might be driven by the reshaping of microbial communities, which are strongly affected by changes in the soil physicochemical properties. Our results indicate that drainage is unfavorable in terms of greenhouse gases (GHGs) emissions in peatlands and that rewetting the Zoige alpine peatlands should be considered as a smart option from a climatic perspective in the future.

1. Introduction

Peatlands are unique habitats that only cover approximately 3% of the global land area, yet hold approximately-one-third of the total global soil C (Wilson et al., 2016) and large stocks of organic N (Hugelius et al., 2020). Unfortunately, during the last century, 10%–20% of the original peatland area has been drained for agricultural and industrial use (Maljanen et al., 2010). Serious concerns have been raised that such a disturbance could stimulate sequestrated C and N losses, as the soils are no longer protected by anaerobic conditions, and subsequently trigger carbon dioxide (CO_2) and nitrous oxide (N_2O) emissions, which may further accelerate global warming (Petrescu et al., 2015; Pärn et al., 2018). Among the different greenhouse gases (GHGs), N_2O is known to be an important peatland-related GHG owing to its large warming

* Corresponding author at: Beijing Key Laboratory of Biodiversity and Organic Farming, College of Resources and Environmental Sciences, China Agricultural University, Beijing 100193, China.
E-mail address: d.wu@cau.edu.cn (D. Wu).

https://doi.org/10.1016/j.geoderma.2022.116206
Received 28 June 2022; Received in revised form 26 September 2022; Accepted 29 September 2022
Available online 22 October 2022

potential, radiative efficiency, and ozone-depleting capacity (Bouwman et al., 2002; Ravishankara et al., 2009). Two key biochemical processes, nitrification and denitrification, control the N_2O production in peatland ecosystems. Nitrifying bacteria produce N_2O as a byproduct of NH_3 oxidation, whereas denitrifiers produce N_2O as an obligate intermediate in the production of N_2 (Braker and Conrad, 2011; Butterbach-Bahl et al., 2013). Owing to the higher soil moisture and labile C content, denitrification is believed to be the major N loss process and the dominant source of N_2O emissions in peatlands (Salm et al., 2012; Gil et al., 2017). However, it has also been reported in an earlier study that a lack of N_2O production, rather than N_2O consumption, represent error around zero in peatland soils (Hayden and Ross, 2005). This is possibly because denitrification is not only the source of N_2O but also a significant biological sink for N_2O through the N_2O reduction to N_2 process. Indeed, nitrate is often found to be a limiting factor for denitrification in peatlands (Davidsson et al., 2002), whereas a higher N_2O reduction to N_2 process would be specifically enhanced under low NO_3^- conditions with a high denitrification rate (Blackmer and Bremner, 1978; Senbayram et al., 2019).

Long-term drainage in peatlands reshapes soil physicochemical characteristics, plant species, and soil microbial diversity, which affects N_2O emissions in various ways (Wang et al., 2019; Xu et al., 2021). Artificial drainage affects community structure and composition both above- and below-ground in peatlands (Leroy et al., 2018). Higher plant species diversity and more complex microbial interactions are often observed in drainage peatlands (Murphy et al., 2009; Qiao et al., 2014; Zeng et al., 2021). However, how these changes affect the soil N cycle and N_2O emissions within it remains unclear. Peatland drainage typically increases the bulk density of peat soil through the shrinkage of organic peat fibers and compaction (Ali et al., 2006; Hooijer et al., 2012; Könönen et al., 2015). Increasing soil bulk density causes a decline in soil relative gas diffusivity and a reduction in soil oxygen supply, which may favor denitrification-derived N_2O (van Groenigen et al., 2005; Rousset et al., 2020; Yang et al., 2022). However, when ditches are dug for drainage, the highly decomposed peat soil is often saturated after rainfall events and quickly drains again (Wang et al., 2019). Such a drying-rewetting cycle drives a quick soil O_2 status transition from oxic to anoxic, which is known to trigger high N_2O emissions (Groffman et al., 2009; Harris et al., 2021; Song et al., 2022). Furthermore, long-term drainage could stimulate high nutrient losses, such as dissolved organic carbon (DOC), which affects nitrification and denitrification rates in various ways (Strack et al., 2008; Macrae et al., 2013; Wu et al., 2017b). A greater understanding of the effects of drainage on the N cycle processes that regulate N_2O production and consumption dynamics is important to improve future peatland management for both climate change mitigation and adaptation in alpine peatlands. However, much of the work to date on drainage-induced changes in peatland N_2O emissions is based on field observations, where quantification of N_2O consumption is still not possible because of the high background atmospheric N_2 concentration (Butterbach-Bahl and Dannenmann, 2011; Wu et al., 2017a; Senbayram et al., 2018). Previous laboratory studies investigating denitrification have often used the classical acetylene inhibition method, which is now considered unsuitable for quantifying denitrification rates because of a range of inevitable artefacts such as catalytic NO decomposition (Groffman et al., 2006; Nadeem et al., 2013). In recent decades, robotic incubation systems have been developed using a helium (He) atmosphere with real-time monitoring and quantification of N_2 and N_2O emissions, allowing for a full assessment of soil ecosystem N losses (Cárdenas et al., 2003; Senbayram et al., 2018). Furthermore, the ^{15}N-N_2O site-preference (SP) approach has been widely used to distinguish the different sources of N_2O production pathways [+34‰ to +40‰ for nitrification (Ni) and fungal denitrification (fD), −9‰ to +9‰ for bacterial denitrification (bD)] (Decock and Six, 2013; Toyoda et al., 2017). The combination of a robotic He atmosphere incubation system with a SP approach has been proven to be a powerful tool for N_2O source partitioning (Wu et al., 2019; Senbayram et al., 2020).

Among the different types of peatlands, alpine peatlands are known to be the most susceptible to climate change due to their intrinsic low temperature (Braker and Conrad, 2011). The Zoige peatland, which is located in the sensitive region at the eastern margin of the Qinghai-Tibet Plateau (QTP), is the largest alpine peatland region in the world, with a total area of 4605 km^2 and 3500 m above sea level (Chen et al., 2014; Xue et al., 2021). From the 1950s to the 1970s, more than 1600 artificial ditches were dug to enlarge rangelands, leading to a significant decrease in water table levels in 40% of the total area of the Zoige peatland (Xiang et al., 2009; Li et al., 2018; Wei et al., 2018). The response of N_2O emissions to drainage might be different from that of other peatlands because of the lower atmospheric O_2 content (14%). However, little research has been undertaken to understand the underlying mechanisms of drainage on the N cycle related processes and N_2O emissions in this region, especially at an N_2O emission "hot moment" event that contributes substantially to overall emissions (Li et al., 2015; Lee et al., 2017). In this study, we chose two adjoining sites in the Zoige peatland that include one natural peatland and one that has been artificially drained for more than 50 years. We first investigated the effects of drainage on soil properties and above- and belowground community compositions in peatlands. Furthermore, we combined the SP isotopic mapping approach with qPCR and high-throughput 16S rRNA gene sequencing and conducted incubation experiments using a robotized continuous flow system under an He/O_2 atmosphere robotized incubation system. Based on a direct comparison between natural and artificially drained peatlands, we hypothesized that: (i) long-term drainage increases both aboveground plant species diversity and belowground microbial diversity. (ii) Denitrification is the dominant source of N_2O emitted by soil in both soils owing to its intrinsically low O_2 content. (iii) Drainage peatlands have lower N_2O emissions during the N_2O hot moment events due to nutritional losses.

2. Material and methods

2.1. Soil sampling sites

Annual precipitation in the Zoige peatland (3500 m a.s.l.) varied from 464 mm to 862 mm over the period from 1961 to 2015 (the average was 653 mm), 52.5% of which occurred from July to September. The mean annual air temperature was 1.3°C, with the lowest mean monthly record in January (-14.1°C, 1963) and the highest mean monthly record in July (13.5°C, 2010). Meteorological data for the Zoige peatland were obtained from the China National Meteorological Information Center. The soil texture is classified as silty loam (Zhang et al., 2018). The main vegetation types are *Kobresia humilis*, *Scirpus pumilus*, *Kobresia pygmaea*, *Kobresia setchwanensis*, and *Carex muliensis* (Cao et al., 2017). Soil was collected from an alpine peatland in the Zoige peatland. Two sampling sites were used, including the natural alpine peatland site (33.92°N, 102.82°E) and an artificial drainage peatland site (33.91°N, 102.74°E). Most ditches have been excavated for drainage in the Zoige peatland since the 1950s (Wei et al., 2018) and have similar physical features, that is, 1–2 m width, 62–18,008 m length, and 0–0.224 slopes (Li et al., 2018). From July to September, water table depth from surface ranged between 20 cm and 40 cm on average in natural alpine peatland (Xiang et al., 2009), while in the artificially drained peatland, the water table declined.

2.2. Plant species composition and biomass

Before collecting the soil samples, we randomly selected 45 plots (1 m × 1 m) within natural alpine peatlands and artificial peatlands. Any two plots were separated by at least 5 m. For each plot, we first investigated the number of plant species and species richness and then harvested the aboveground plant biomass. The aboveground plant biomass was dried at 70°C for 48 h and then weighed. Plant total C and N were

measured using an element analyzer (Flash 2000, Thermo, USA).

2.3. Incubation experimental design

Five replicate sets of soil samples (0–30 cm) were collected by a peat auger from random points within each site, with a distance between adjacent plots of at least 30 m, and then mixed to homogenise it completely once after collection. The collected soils were air-dried and sieved to a particle size of 1 mm, and the root and plant residues were manually removed, and stored in sealed sterile bags. The incubation experiment was carried out at the China Agricultural University in a robotized continuous-flow incubation system (ROFLOW) (Senbayram et al., 2018). The experiment consisted of two soils (a natural alpine peatland and an artificial drainage peatland). The soils were pre-incubated for 3 days in a 45% water-filled pore space (WFPS) before the incubation experiment. Afterwards, soils (1.0 kg dry weight) were packed into incubation vessel (with inner diameters of 130 mm and heights of 180 mm) with three replicates at a bulk density (BD) of ca. 0.4 g cm^{-3} (natural peatland) and 0.6 g cm^{-3} (drained peatland), which corresponded to the real soil BD in the field, and soil moisture was adjusted to 60% WFPS. The WFPS (45% in pre-incubation and 60% in experiment) selected in this study was determined according to the previous study (average 40%–60% over the year-round period, Zhang et al., 2018) and the measured results of collecting soil sample in this study (50%–60%). The incubation vessels were sealed and the atmospheric air in the vessels were washed with 100% ultra-high-purity He by repeated evacuation for three cycles, to remove N_2 in the vessels. The incubation atmosphere was continuously flushed with a He and O_2 (86:14 v/v) mixture to simulate the actual atmospheric conditions of the Zoige peatland (Wang et al., 2017). The temperature of the incubation vessel was set at 20 ± 1°C. The incubation experiments included three successive events: a rewetting event – increasing soil WFPS to 60%; N deposition event – equivalent to 100 kg N ha^{-1} (NH_4^+: NO_3^-=1:1) was thoroughly dissolved in 20 ml deionized water and then spread on the soil surface using a syringe; oxic to anoxic transition event – changing the incubation atmosphere from 14% O_2 to 0% O_2 (He: O_2 = 100%:0%).

2.4. Gas and soil measurements

Gas concentrations (i.e., N_2O, N_2, O_2, and CO_2) were monitored in real time and analyzed using a gas chromatograph (Agilent Technologies Inc., SCLA, Ca, USA) equipped with a pulsed discharge helium ionization detector (PDHID). The flux rate of the gas was determined by the flow rate and concentration difference between the inlet and outlet of the incubation vessel (Lindsay et al., 2010). Soil total carbon (TC) and total nitrogen (TN) were measured using an element analyzer (Flash 2000, Thermo, USA). Soil organic carbon (SOC) and Dissolved organic carbon (DOC) were determined via dry combustion using a vario TOC select elementar and an Elementar Vario Max CN analyzer (Hanau, Germany), respectively. The concentrations of NO_3^- and NH_4^+ in the soil were analyzed using a continuous flow analyzer (TRAACS2000, Bran + Luebbe Co. ltd., Hamburg, Germany) after extraction with a 1 M KCl solution. The soil pH in each vessel was measured in water (1:5, w/v).

2.5. Isotope analysis

The $\delta^{15}N^{bulk}$, $\delta^{15}N^{\alpha}$, and $\delta^{18}O$ isotope signatures of N_2O were then determined by analyzing *m/z* 44, 45, and 46 of intact N_2O^+ molecular ions and *m/z* 30 and 31 of NO^+ fragment ions (Orellana et al., 2012) using an isotope ratio mass spectrometer (Isoprime100, Isoprime, Cheadle, UK). The $\delta^{15}N$ value at the terminal position of the N_2O molecule, $\delta^{15}N^{\beta}$, was calculated using the following equation (Tang et al., 2019):

$$\delta^{15}N^{\beta} = 2 \bullet \delta^{15}N^{bulk} - \delta^{15}N^{\alpha} \quad (1)$$

The isotope effects during N_2O reduction and the ^{15}N site preference (SP value) of the initial substrate (SP_0) were calculated using a Rayleigh-type model, assuming that the isotope dynamics followed closed-system behavior.

$$SP_{N_2O-r} = SP_{N_2O-0} + \eta_r \ln\left(\frac{C}{C_0}\right) \quad (2)$$

Where SP_{N_2O-r} is the SP value of the remaining substrate. SP_{N_2O-0} is the SP value of the initial substrate. η_r is the net isotope effect (NIE) associated with N_2O reduction, and C and C_0 are the residual and initial substrate concentrations, respectively, that is, the expression (C/C_0) represents the product ratio ($N_2O/(N_2O + N_2)$).

Source partitioning of N_2O production was based on the two-end-member isotopic mass balance equation:

$$SP_{N_2O-0} = SP_D \times f_{D-SP} + SP_N \times f_{N-SP} \quad (3)$$

In this equation, SP_D and SP_N represent the SP value of bacterial denitrification/nitrifier denitrification and nitrification/fungal denitrification, respectively. f_{D-SP} and f_{N-SP} is the contribution of bacterial denitrification/nitrifier denitrification and nitrification/fungal denitrification to total N_2O release calculated on the basis of SP values, respectively. It is assumed that we deal with only two end members; hence, $f_{D\text{-}SP} + f_{N\text{-}SP} = 1$. Distinguishing N_2O originating from fungal denitrification and bacterial nitrification or between bacterial denitrification and nitrifier denitrification based on SP values is mathematically impossible because of the overlapping SP values. Therefore, the isotopic signatures of the end members were defined as 37‰ for both bacterial nitrification and fungal denitrification and –2‰ for bacterial denitrification and nitrifier denitrification (Decock and Six, 2013; Toyoda et al., 2017). In this equation, $f_{D\text{-}SP}$ and $f_{N\text{-}SP}$ represent the contribution of denitrification and nitrification/fungal denitrification to the total N_2O release calculated based on SP values, respectively.

2.6. Quantification of functional gene copies and high-throughput sequencing of 16S rRNA gene amplicons

The soil samples were frozen in a refrigerator at −80°C before DNA extraction. DNA was extracted from the frozen soil using the FastDNA SPIN Kit for soil (MP Biomedicals, Santa Ana, CA, USA). A NanoDrop 2000 UV–Vis spectrophotometer (Thermo Fisher, USA) was used to assess DNA quality. The functional gene abundance of *nirK*, *nirS*, and *nosZ* was quantified in triplicate by real-time PCR using an iCycler IQ (Biorad, USA). The qPCR assay for standards, samples, and no-template control was performed in triplicate on an Applied Biosystems 7500 Real-Time PCR System (Thermo Fisher Scientific, USA) in a 96-well format. The thermal conditions were summarized as follows: the 20 μL reaction mixture contained 10 μL of SYBR Premix Ex Taq (Tli RNase H Plus; 2 × concentration) from TaKaRa (Shiga, Japan); 0.5 μL of each 10 μmol/L primer, 7 μL of sterile DNase-free water, and 2 μL of DNA or sterile DNase-free water. The PCR test was performed under the following conditions: 95°C for 30 s, followed by 40 cycles at 95°C for 5 s, 60°C for 40 s, and 72°C for 20 s. The fluorescence signal was acquired after the extension phase of each cycle at 72°C. Melting curve analysis was performed to determine the specificity of the products. PCR products that had been resolved on a 1% agarose gel were checked after ethidium bromide staining to confirm the specificity of the amplification. The abundance of functional genes was calculated as a copy number per gram of dry soil.

The V4-V5 region of the 16S rRNA gene was amplified using PCR testing. The PCR program was performed under the following conditions: 94°C for 5 min, 30 cycles (94°C for 30 s, 55°C for 30 s, 72°C for 45 s), and a final extension at 72°C for 10 min. The Illumina MiSeq platform (Illumina, San Diego, USA) was used for high-throughput sequencing (Wu et al., 2021). After sequencing, sequences shorter than 200 Base Pair (bp) and with a quality score < 25 were excluded and then assigned to soil samples based on the unique barcode using the Quantitative

Table 1
Properties of the soil (0–30 cm) and plant community indexes in Zoige peatland. Different letters indicate significant differences between natural alpine peatland and artificial drainage peatland ($P < 0.05$). Data are mean ± standard error (n = 3).

	Natural alpine peatland	Artificial drainage peatland
Soil properties		
Total C (g C kg^{-1} soil)	121.8 ± 1.39a	114.8 ± 0.95b
Total N (g N kg^{-1} soil)	9.79 ± 0.08	9.59 ± 0.05
Soil organic carbon (SOC, g C kg^{-1} soil)	110.6 ± 4.52	109.7 ± 5.26
Dissolved organic carbon (DOC, mg C kg^{-1} soil)	12.1 ± 0.09a	10.6 ± 0.62b
NO_3^- (mg N kg^{-1} soil)	67.6 ± 1.97b	82.6 ± 1.62a
NH_4^+ (mg N kg^{-1} soil)	19.3 ± 4.07	7.87 ± 2.50
pH	7.80 ± 0.05	7.83 ± 0.03
C/N	11.3 ± 0.47	11.4 ± 0.49
Bulk density (BD, g cm^{-3})	0.41 ± 0.03b	0.61 ± 0.03a
Sand (%)	63.1	53.8
Silty (%)	24.5	33.6
Clay (%)	12.4	12.6
Plant community indexes		
Average number of species (m^{-2})	5.29 ± 0.20	6.02 ± 0.38
Plant density (plant m^{-2})	301 ± 19.4a	185 ± 10.0b
Shannon-Wiener index	1.03 ± 0.04b	1.31 ± 0.06a
Simpson index	0.53 ± 0.02b	0.64 ± 0.02a
Margalef abundance index	0.77 ± 0.04b	0.97 ± 0.07a
Pielou evenness index	0.63 ± 0.02b	0.77 ± 0.02a
Aboveground Biomass (g m^{-2})	443 ± 53.2	364 ± 44.0
C content (mg g^{-1})	430 ± 4.66a	381 ± 6.49b
N content (mg g^{-1})	18.6 ± 0.61	21.7 ± 2.41
P content (mg g^{-1})	1.86 ± 0.19	1.29 ± 0.15
Plant density (plant m^{-2})		
Poaceae	9.29 ± 3.72	35.2 ± 5.23
Cyperaceae	200.8 ± 14.4	50.9 ± 7.71
Rosaceae	51.0 ± 4.44	30.8 ± 3.37
Others	40.0 ± 1.93	68.4 ± 3.12
Coverage (%)		
Poaceae	4.76 ± 1.67	22.8 ± 3.37
Cyperaceae	61.7 ± 3.91	25.2 ± 3.80
Rosaceae	31.6 ± 3.06	27.4 ± 4.51
Others	23.4 ± 1.16	45.6 ± 2.23

Insights into Microbial Ecology pipeline (QIIME, version 1.17; Caporaso et al., 2010). Operational taxonomic units (OTUs) were generated at a 97% identity threshold, and the most abundant sequence was chosen as a representative sequence of each OTU. Taxonomy was then assigned to OTUs with reference to a subset of the SILVA 119 database (https://www.arb-silva.de/download/archive/qiime/). All samples were then rarefied to 180,000 sequences per sample to evaluate bacterial diversity, which allowed us to compare the general diversity patterns among treatments. See Supplementary Information and Supplementary Table S1 for the primer sets.

2.7. Statistical analysis

All data is presented as the mean ± SE. The cumulative gas emissions were calculated by linear interpolation between the measured fluxes. Significance statistics were carried out by *t* test ($P < 0.05$), following the homogeneity of variance and the tests of assumptions of normal distribution. Plant community indexes, such as the Shannon-Wiener index, Simpson index, Margalef abundance index, and Pielou evenness index, were calculated using the vegan package in R (version 4.1.1). The resulting OTU table was used in all subsequent statistical analyses of differentially abundant taxa as well as analyses of α- and β-diversity. Networks were visualized with the Gephi version 0.9.1 software package. The heatmap was performed to reveal the relationships between the main microbial phyla and soil properties using the pheatmap package in R (version 4.1.1). Venn diagrams were conducted using the ggvenn package in R (version 4.1.1) to perform the differences of microbial OTUs from two soils. All statistical analyses were performed using SPSS 22.0 (SPSS Inc., Chicago, IL, USA). Graphs were prepared using OriginPro 9.1 (Origin Lab Corporation, Northampton, MA, USA).

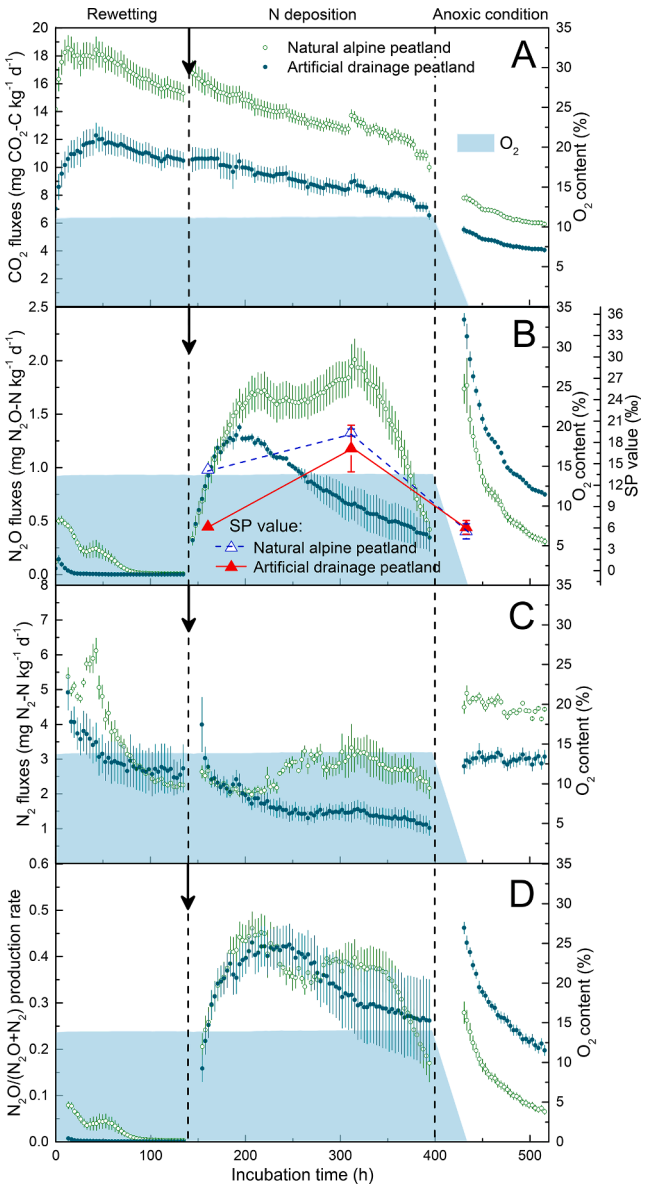

Fig. 1. CO_2, N_2O, N_2 fluxes and $N_2O/(N_2O + N_2)$ production ratio of natural alpine peatland and artificial drainage peatland during incubation time. Black solid arrow indicates N deposition. Error bars show the standard error of the mean value (n = 3). There is no data from 400 to 430 h due to equipment malfunction.

3. Results

3.1. Soil properties and plant community indexes

The natural alpine peatland had an initially higher TC and DOC compared with the drainage peatland, while the drainage peatland had a higher NO_3^- concentration and bulk density ($P < 0.05$, Table 1). With long-term drainage, the density and coverage of Cyperaceae and Rosaceae decreased, whereas Poaceae and others began to occur more frequently (Table 1). Long-term drainage led to a significant increase in most plant diversity indexes ($P < 0.05$; Table 1).

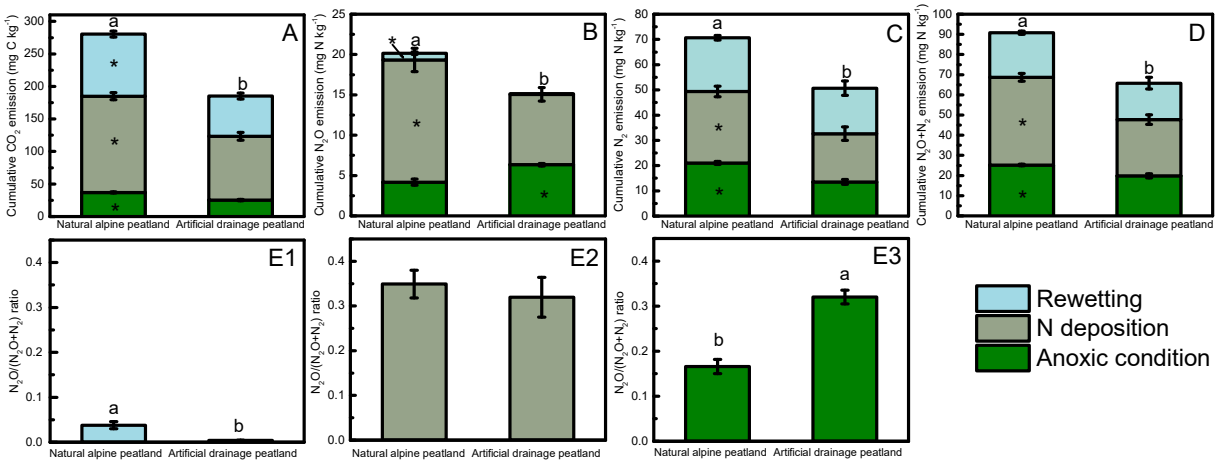

Fig. 2. Cumulative CO_2 (A), N_2O (B), N_2 (C), and $N_2O + N_2$ (D) emissions and $N_2O/(N_2O + N_2)$ ratio (E1-3) during different Event in natural alpine peatland and artificial drained peatland. Different letters and * indicate significant differences in total emissions and in each event between two soils ($P < 0.05$), respectively. Data are mean ± standard error (n = 3).

Table 2
Nitrification/fungal denitrification proportion calculated on the basis of N_2O SP values and the two-end-member model in natural alpine peatland and artificial drainage peatland.

			Natural alpine peatland	Artificial drainage peatland
N deposition	First time	Min	0%	0%
		Median	50.2%	25.7%
		Max	100%	87.8%
	Second time	Min	32.2%	6.90%
		Median	66.3%±3.8%	59.4%±6.1%
		Max	100%	100%
Anoxic condition	Third time	Min	0%	0%
		Median	23.8%±2.9%	25.5%±2.9%
		Max	93.4%	95.0%

Tables 2 calculated the contribution of nitrification/fungal denitrification on the basis of parameters from Sutka et al. (2006), Lewicka-Szczebak et al. (2017), and Wu et al. (2019), include the weighted median and the range of SP of bacterial denitrification and nitrification/fungal denitrification (‰).

3.2. Gas emissions

The maximum CO_2 flux from natural peatland and drainage peatland was observed after the onset of the experiment (18.4 ± 0.93 mg CO_2-C kg^{-1} vs 12.3 ± 0.90 mg CO_2-C kg^{-1}), and decreased gradually until the end; and a higher flux was observed immediately after N addition in natural peatland (Fig. 1A). The cumulative CO_2 emissions in the natural peatland were 54.0%, 51.0%, 46.1%, and 51.3% higher than those in the drainage peatland during the three events and total cumulative emissions, respectively ($P < 0.05$, Fig. 2A).

During the rewetting event, natural alpine peatlands had higher N_2O and N_2 fluxes than drainage peatlands (Fig. 1B and 1C). Cumulative N_2O emissions in the natural alpine peatland were 11 times higher than those in the drainage peatland during the rewetting event ($P < 0.05$, Fig. 2B). During the N input event, the N_2O fluxes showed a trend similar to that of the rewetting event (Fig. 1B). The N_2 fluxes of the drainage peatlands were always lower than those of the natural peatlands (Fig. 1C). Cumulative N_2O and N_2 emissions in the natural peatland were 74.3% and 48.2% higher than those in the drainage peatland, respectively ($P < 0.05$, Fig. 2B and 2C). N_2O and N_2 fluxes were triggered by an oxic-to-anoxic transition event, with a higher N_2O emission and lower N_2 emission observed in the drainage peatland (Figs. 1 and 2). A higher $N_2O/(N_2O + N_2)$ ratio was observed in natural peat soil than in drainage peat soil during rewetting and N deposition events, whereas the opposite

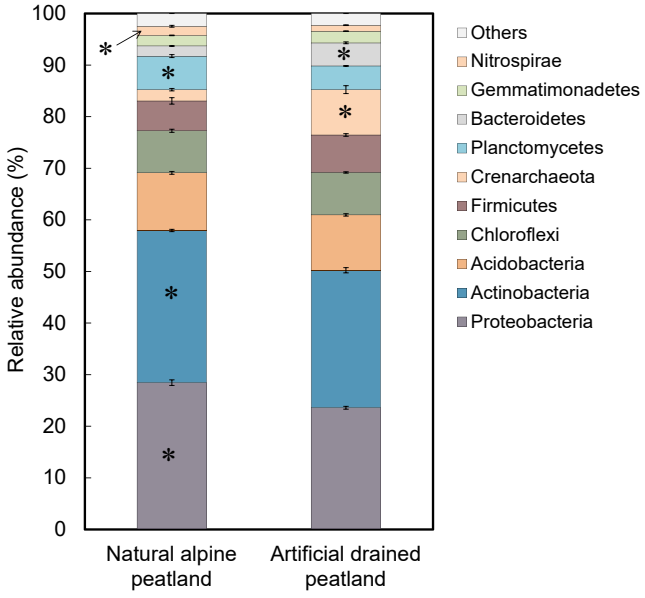

Fig. 3. The proportional abundance of microbial dominant phyla from natural alpine peatland and artificial drainage peatland. * indicate significant difference between natural alpine peatland and artificial drainage peatland ($P < 0.05$). Error bars show the standard error of the mean value (n = 3).

Table 3
Numbers of OTUs, Shannon and Simpson biodiversity indexes of 16S rRNA of soil samples in Zoige peatland. Different letters indicate significant difference between natural alpine peatland and artificial drained peatland ($P < 0.05$). Data are mean ± standard error (n = 3).

	Natural alpine peatland	Artificial drainage peatland
PD	226 ± 5.68	230 ± 3.77
Chao1	3675 ± 79.1	3835 ± 97.2
Observed OTUs	3059 ± 53	3162 ± 42
Shannon-Wiener index	8.83 ± 0.02b	9.11 ± 0.02a
Simpson index	0.98 ± 0.00b	0.99 ± 0.00a

PD, Phylogenetic diversity index; Chao 1, Chao1 richness index. The diversity indexes were calculated using 180,000 randomly selected sequences per sample. Different letters indicate significant difference between natural alpine peatland and artificial drainage peatland.

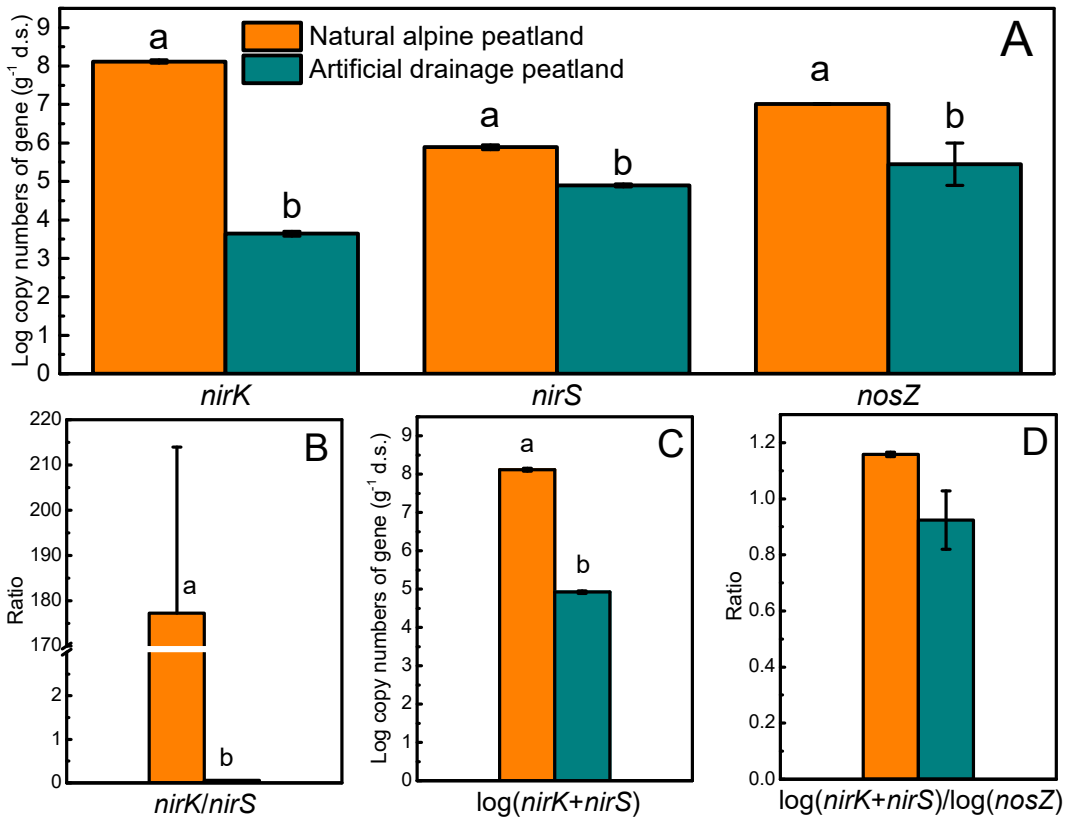

Fig. 4. Abundance of copy numbers of (A): log(*nirK*), log(*nirS*), log(*nosZ*), (B): *nirK*/*nirS*, (C): log (*nirK* + *nirS*), and (D): log (*nirK* + *nirS*)/log (nosZ) for natural alpine peatland and artificial drainage peatland. Different lowercase letters indicate significant differences between natural alpine peatland and artificial drainage peatland ($P < 0.05$). Error bars show the standard error of the mean value (n = 3).

was observed during anoxic events (Fig. 1D and 2E).

3.3. Isotopic signatures of soil-emitted N_2O and source partitioning

In general, in both natural peatlands and drainage peatlands, the $\delta^{15}N^{bulk}$ and $\delta^{18}O$ values of soil-emitted N_2O increased with time during the N deposition event and then decreased during the oxic to anoxic transition (Fig. S1). The $\delta^{15}N^{bulk}$ and $\delta^{18}O$ values in the natural peatland were higher than those in the drainage peatland, except for the $\delta^{18}O$ value in the second sampling period (Fig. S1). In the endmember map with $\delta^{18}O$ versus SP values, the second sampling data points were generally far away from the reduction line within the nitrification/fungal denitrification source area (Fig. S2).

The SP values ranged from 4.20‰ to 21.5‰ in the natural peatland and from 4.92‰ to 20.8‰ in the long-term drainage peatland (Fig. S1). Based on the SP values and the two-end-member mixing model, the soil-emitted N_2O of the first emission peak was mainly produced by the mixture source (≈50% each, nitrification and denitrification) in the natural peatland and the denitrification pathway (≈74.3%) in the drainage peatland during the N deposition event, and the nitrification process was the main N_2O source in the second sampling time (Table 2). Most of the soil-emitted N_2O was produced by denitrification in the oxic to anoxic transition event (Table 2 and Fig. S2). The isotopic signature of emitted N_2O during the rewetting event is not shown, as the N_2O concentration was too low for the accurate determination of its isotopic values.

3.4. Diversity, functional gene abundance, relative abundance and relationships between soil properties and microbial dominant phylum

In this study, the most abundant bacterial phyla (> 1%) accounted for > 97% of the bacterial community (Fig. 3). Compared with drainage peatlands, natural peatlands showed a greater relative abundance of Proteobacteria, Actinobacteria, Planctomycetes, and Nitrospirae, and a lower relative abundance of Crenarchaeota and Bacteroidetes ($P < 0.05$, Fig. 3). The Shannon and Simpson indices of drainage peatlands were significantly higher than those of natural peatlands ($P < 0.05$), whereas no differences were found in other indices (Table 3). Natural peatlands had higher denitrification functional gene copy numbers, ratios of *nirK*/*nirS* and log (*nirK* + *nirS*) compared with drainage peatlands ($P < 0.05$, Fig. 4).

The natural soil and drainage soil shared 2834 OTUs (41.3%), whereas the drainage peatland soil had 2095 unique OTUs (Fig. S3). The overall network of bacterial phyla in soil samples revealed a total of 486 connections, which were identified in natural peatland, including 265 (54.5%) inferred positive interactions and 221 (45.5%) inferred negative interactions (Fig. 5). The natural peatland network contained higher nodes and higher average geodesic distances while exhibiting a lower average node degree and lower average clustering coefficients than the drainage peatland (Fig. 5 and Table S2). Soil NO_3^- concentration was positively correlated with Crenarchaeota and Bacteroidetes, and negatively correlated with Proteobacteria, Actinobacteria and Planctomycetes ($P < 0.05$), whereas the opposite results were found for other indices, such as NH_4^+, TN, DOC, and TC (Fig. 6). SOC and C/N ratio had no significant effects on the dominant microbial phyla (Fig. 6).

4. Discussion

Hot-moment events, including rewetting, N input, and oxic-to-anoxic transition, are known to contribute markedly to the overall soil N_2O emissions in peatlands (Lee et al., 2017; Harris et al., 2021 Song et al., 2022). Contrasting N_2O and N_2 flux patterns were observed between

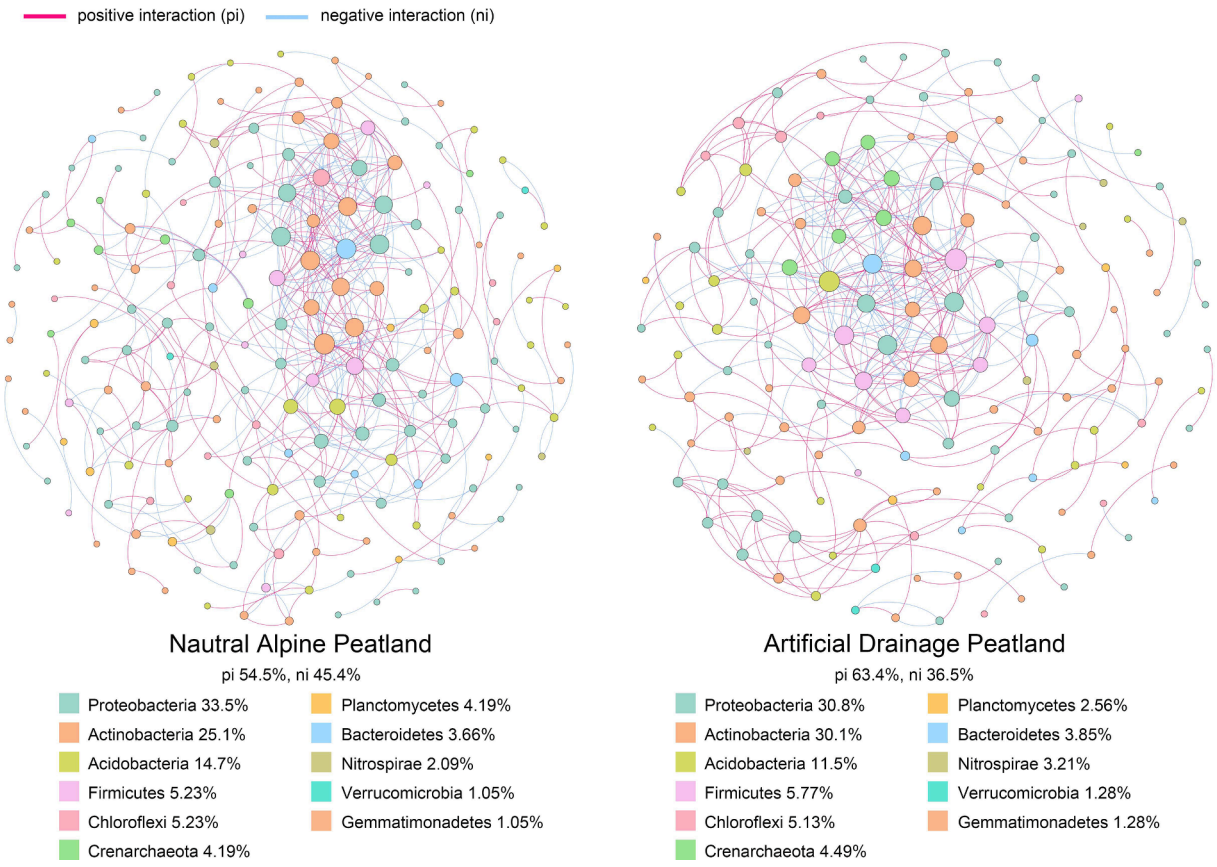

Fig. 5. Network interactions showing relationships among bacterial phylum at natural alpine peatland and artificial drainage peatland, respectively. Different node colors indicate different predominant phyla, as indicated below the networks. Red connections show positive correlations between two individual nodes and blue connections show negative correlations between nodes. The size of each node is proportional to its degree.

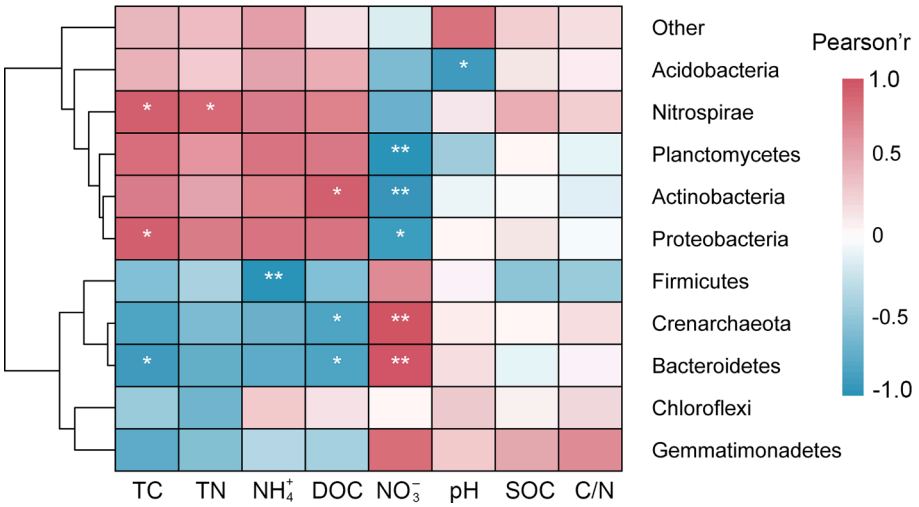

Fig. 6. Heatmap showing the correlation between soil properties and the main microbial phyla. * and ** indicate significant correlations at $P < 0.05$ and 0.01, respectively. TC, total carbon; TN, total nitrogen; DOC, dissolved organic carbon; SOC, soil organic carbon.

natural and drainage peatlands in response to hot-moment events (Fig. 1), indicating the complex impacts of drainage on N_2O production and consumption processes in peatlands. In line with previous studies (Murphy et al., 2009; Qiao et al., 2014; Zeng et al., 2021), we found that drainage increased plant diversity in peatlands (Table 1), which is likely due to the succession of plant species from aquatic plants to terrestrial plants (Rinnan et al., 2007; Wertz et al., 2009). Plant diversity has been reported to decrease N_2O emissions under nitrogen-limited conditions (Niklaus et al., 2016), which is consistent with the considerably lower N_2O fluxes in the drainage peatlands observed in our study after rewetting and N addition (Fig. 1). However, some studies have also found that high plant diversity and richness enhance both N_2O and CO_2 emissions due to increased soil moisture and carbon input (Regina et al., 1998; Sun et al., 2013; Niklaus et al., 2016). This discrepancy is possibly due to the potentially different responses of plant species to rewetting/N addition. A significant decline of CO_2 fluxes after N loading were

observed, which could be due to the inhibition effect of N addition on soil respiration (Ramirez et al., 2010) and decreased DOC content during incubation. The bulk density in drainage soil was much higher than that in natural soil (0.6 vs 0.4 g cm^{-3}), which is consistent with previous studies that found that peatland degradation typically increases the bulk density of peat soil through shrinkage of the organic peat fibers and compaction (Könönen et al., 2015; Liu et al., 2019). The higher bulk density in drainage soil led to lower soil gas diffusivity and aeration compared to natural soil, which would increase the proportion of denitrification-derived N_2O (Rousset et al., 2020; Yang et al., 2022). This is supported by the N_2O ^{15}N site preference value observed during the oxic phase, which suggests that nitrification was the dominant source of N_2O emissions in natural soil, while the majority of soil-emitted N_2O in the drainage peatland was produced by denitrification (Table 2).

Under anoxic conditions, natural soil showed a markedly higher denitrification rate than drainage soil (5.24 ± 0.08 vs 4.22 ± 0.20 mg N kg^{-1} day^{-1}). This is further supported by the higher denitrification functional gene abundance observed in natural soil, indicating that long-term drainage decreased the denitrification potential (Xue et al., 2021). The lower denitrification rate in drainage soil is possibly due to long-term drainage caused by a lower labile C in the soil (Xue et al., 2021), as indicated by the considerably lower CO_2 fluxes observed in the drainage peatland (Fig. 1). This is supported by the lower TC and DOC in drainage peatlands compared to natural peatlands, implying accelerated C decomposition in peat and degradation in drainage soil (Krüger et al., 2015; Urbanová and Bárta, 2016). Interestingly, instead of a lower N_2O emission, the drainage peatland showed a higher N_2O emission and a much lower N_2 production rate during the anoxic phase compared with natural soil (Figs. 1 and 2). As a non-significant difference between drainage and natural soil was observed on log (*nirK* + *nirS*)/log (*nosZ*) (Fig. 4), we speculate that this is possibly because the high DOC content and low nitrate availability of natural peatland promoted N_2O reduction to N_2 (Kandeler et al., 2006; Long et al., 2017).

Apart from aboveground plant succession, long-term drainage also drives soil microbial activities towards aerobic processes (Espenberg et al., 2018), which accelerates peat C decomposition and soil degradation due to persistent aerobic conditions (Fenner and Freeman, 2011; Liu et al., 2018). Natural and drainage peatland soils shared only 41.3% OTUs of the total OTUs, indicating a significant shift in the microbial composition after long-term drainage (Urbanová and Bárta, 2016). The drainage peatland showed a higher Shannon and Simpson biodiversity index than the natural peatland (Table 3, Fig. 5), implying that long-term drainage increased soil microbial diversity (Urbanová and Bárta, 2016). As shown in Fig. 6, soil properties such as NO_3^-, DOC, and TC strongly affected the microbial community structure. Furthermore, NO_3^- concentrations were significantly correlated with Actinobacteria and Proteobacteria (organic matter decomposers), and the network interaction showed that these two phyla were interconnected in peatland soils (Fig. 5), implying that NO_3^- content is a primary soil physicochemical property influencing microbial community composition (Kraft et al., 2011). Since important ecosystem services are provided by healthy peatlands (Marsden and Ebmeier, 2012), considerable efforts have been made worldwide in the last few decades to rewet peatlands by installing dams, refilling drainage ditches, and pumping water into the peatlands (Thom et al., 2019). Recent analysis suggests that the restoration of drained peatlands is the most resource-efficient way to improve soil carbon sequestration (Leifeld and Menichetti, 2018). With the growing public awareness of environmental protection and social development in recent years, rewetting of the Zoige peatland (e.g., protection strategies) is expected in the coming decades. Based on this study, we showed that drainage altered the product stoichiometry of denitrification in the Zoige alpine peatlands in an unfavorable way in terms of N_2O mitigation. Thus, rewetting the Zoige alpine peatland should be considered as a climate-smart option. Recent studies suggest that rewetting might mitigate N_2O emissions in peatlands (Liu et al., 2020; Minkkinen et al., 2020; Lin et al., 2022). Nevertheless, given that the changes in surface vegetation and soil chemistry that govern the microbial community response may take years to establish after a change in the water table level, it is important to evaluate the response of N_2O emissions to rewetting over the long-term.

Declaration of Competing Interest

The authors declare that they have no known competing financial interests or personal relationships that could have appeared to influence the work reported in this paper.

Data availability

Data will be made available on request.

Acknowledgments

This study was supported by The National Nonprofit Institute Research Grant (No. CAFYBB2019SY035), The High-end Foreign Experts Program (No. G2021057003L), and National Natural Science Foundation of China (Nos. 42077037, 41907024).

Appendix A. Supplementary data

Supplementary data to this article can be found online at https://doi.org/10.1016/j.geoderma.2022.116206.

References

Blackmer, A.M., Bremner, J.M., 1978. Inhibitory effect of nitrate on reduction of N_2O to N_2 by soil-microorganisms. Soil Biol. Biochem. 10 (3), 187–191. https://doi.org/10.1016/0038-0717(78)90095-0.

Bouwman, A.F., Boumans, L.J.M., Batjes, N.H., 2002. Emissions of N_2O and NO from fertilized fields: Summary of available measurement data. Global Biogeochem. Cycles 16 (4), 1058. https://doi.org/10.1029/2001GB001811.

Braker, G., Conrad, R., 2011. Diversity, Structure, and Size of N_2O-Producing Microbial Communities in Soils-What Matters for Their Functioning? Adv. Appl. Microbiol. 75, 33–70. https://doi.org/10.1016/B978-0-12-387046-9.00002-5.

Butterbach-Bahl, K., Baggs, E.M., Dannenmann, M., Kiese, R., Zechmeister-Boltenstern, S., 2013. Nitrous oxide emissions from soils: How well do we understand the processes and their controls? Phil. Trans. R. Soc. B 368. https://doi.org/10.1098/rstb.2013.0122.

Butterbach-Bahl, K., Dannenmann, M., 2011. Denitrification and associated soil N_2O emissions due to agricultural activities in a changing climate. Curr. Opin. Env. Sust. 3 (5), 389–395. https://doi.org/10.1016/j.cosust.2011.08.004.

Cao, R., Xi, X., Yang, Y., Wei, X., Wu, X., Sun, S., 2017. The effect of water table decline on soil CO_2 emission of Zoige peatland on eastern Tibetan Plateau: A four-year in situ experimental drainage. Appl. Soil Ecol. 120, 55–61. https://doi.org/10.1016/j.apsoil.2017.07.036.

Caporaso, J.G., Kuczynski, J., Stombaugh, J., Bittinger, K., Bushman, F.D., Costello, E.K., Fierer, N., Peña, A.G., Goodrich, J.K., Gordon, J.I., Huttley, G.A., Kelley, S.T., Knights, D., Koenig, J.E., Ley, R.E., Lozupone, C.A., McDonald, D., Muegge, B.D., Pirrung, M., Reeder, J., Sevinsky, J.R., Turnbaugh, P.J., Walters, W.A., Widmann, J., Yatsunenko, T., Zaneveld, J., Knight, R., 2010. QIIME allows analysis of high-throughput community sequencing data. Nat Methods. 7 (5), 335–336. https://doi.org/10.1038/nmeth.f.303.

Cárdenas, L.M., Hawkins, J.M.B., Chadwick, D., Scholefield, D., 2003. Biogenic gas emissions from soils measured using a new automated laboratory incubation system. Soil Biol. Biochem. 35 (6), 867–870. https://doi.org/10.1016/S0038-0717(03)00092-0.

Chen, H., Yang, G., Peng, C.H., Zhang, Y., Zhu, D., Zhu, Q., Hu, J., Wang, M., Zhan, W., Zhu, E., Bai, Z., Li, W., Wu, N., Wang, Y., Gao, Y., Tian, J., Kang, X., Zhao, X., Wu, J., 2014. The carbon stock of alpine peatlands on the Qinghai-Tibetan Plateau during the Holocene and their future fate. Quat. Sci. Rev. 95, 151–158. https://doi.org/10.1016/j.quascirev.2014.05.003.

Davidsson, T.E., Trepel, M., Schrautzer, J., 2002. Denitrification in drained and rewetted minerotrophic peat soils in Northern Germany (Pohnsdorfer Stauung). J. Plant Nutr. Soil Sci. 165 (2), 199–204. https://doi.org/10.1002/1522-2624(200204)165:2<199::AID-JPLN199>3.0.CO;2-I.

Decock, C., Six, J., 2013. How reliable is the intramolecular distribution of ^{15}N in N_2O to source partition N_2O emitted from soil? Soil Biol. Biochem. 65, 114–127. https://doi.org/10.1016/j.soilbio.2013.05.012.

Espenberg, M., Truu, M., Mander, Ü., Kasak, K., Nõlvak, H., Ligi, T., Oopkaup, K., Maddison, M., Truu, J., 2018. Differences in microbial community structure and nitrogen cycling in natural and drained tropical peatland soils. Sci. Rep. 8 (1), 4742. https://doi.org/10.1038/s41598-018-23032-y.

Fenner, N., Freeman, C., 2011. Drought-induced carbon loss in peatlands. Nat. Geosci. 4 (12), 895–900. https://doi.org/10.1038/ngeo1323.
Gil, J., Pérez, T., Boering, K., Martikainen, P.J., Biasi, C., 2017. Mechanisms responsible for high N_2O emissions from subarctic permafrost peatlands studied via stable isotope techniques: Subarctic Tundra N_2O Stable Isotopes. Global Biogeochem. Cycles 31 (1), 172–189. https://doi.org/10.1002/2015GB005370.
Groffman, P.M., Altabet, M.A., Böhlke, J., Butterbach-Bahl, K., David, M.B., Firestone, M. K., Giblin, A.E., Kana, T.M., Nielsen, L.P., Voytek, M.A., 2006. Methods for Measuring Denitrification: Diverse Approaches to a Difficult Problem. Ecol. Appl. 16 (6), 2091–2122. https://doi.org/10.1890/1051-0761(2006)016[2091:MFMDDA]2.0.CO;2.
Groffman, P.M., Butterbach-Bahl, K., Fulweiler, R.W., Gold, A.J., Morse, J.L., Stander, E. K., Tague, C., Tonitto, C., Vidon, P., 2009. Challenges to Incorporating Spatially and Temporally Explicit Phenomena (Hotspots and Hot Moments) in Denitrification Models. Biogeochemistry 93 (1), 49–77. https://doi.org/10.1007/s10533-008-9277-5.
Harris, E., Diaz-Pines, E., Stoll, E., Schloter, M., Schulz, S., Duffner, C., Li, K., Moore, K.L., Ingrisch, J., Reinthaler, D., Zechmeister-Boltenstern, S., Glatzel, S., Brüggemann, N., Bahn, M., 2021. Denitrifying pathways dominate nitrous oxide emissions from managed grassland during drought and rewetting. Sci. Adv. 7 (6), eabb7118. https://doi.org/10.1126/sciadv.abb7118.
Hayden, M.J., Ross, D.S., 2005. Denitrification as a Nitrogen Removal Mechanism in a Vermont Peatland. J. Environ. Qual. 34 (6), 2052–2061. https://doi.org/10.2134/jeq2004.0449.
Hugelius, G., Loisel, J., Chadburn, S., Jackson, R.B., Jones, M., MacDonald, G., Marushchak, M., Olefeldt, D., Packalen, M., Siewert, M.B., Treat, C., Turetsky, M., Voigt, C., Yu, Z., 2020. Large stocks of peatland carbon and nitrogen are vulnerable to permafrost thaw. Proc. Natl. Acad. Sci. U. S. A. 117 (34), 20438–20446. https://doi.org/10.1073/pnas.1916387117.
Kandeler, E., Deiglmayr, K., Tscherko, D., Bru, D., Philippot, L., 2006. Abundance of *narG*, *nirS*, *nirK*, and *nosZ* Genes of Denitrifying Bacteria during Primary Successions of a Glacier Foreland. Appl. Environ. Microbiol. 72 (9), 5957–5962. https://doi.org/10.1128/AEM.00439-06.
Könönen, M., Jauhiainen, J., Laiho, R., Kusin, K., Vasander, H., 2015. Physical and chemical properties of tropical peat under stabilised land uses. Mires Peat 16 (8), 1–13.
Kraft, B., Strous, M., Tegetmeyer, H.E., 2011. Microbial nitrate respiration-Genes, enzymes and environmental distribution. J Biotechnol 155, 104–117. https://doi.org/10.1016/j.jbiotec.2010.12.025.
Krüger, J.P., Leifeld, J., Glatzel, S., Szidat, S., Alewell, C., 2015. Biogeochemical indicators of peatland degradation-a case study of a temperate bog in northern Germany. Biogeosciences 12, 2861–2871. https://doi.org/10.5194/bg-12-2861-2015.
Lee, A., Winther, M., Priemé, A., Blunier, T., Christensen, S., 2017. Hot spots of N_2O emission move with the seasonally mobile oxic-anoxic interface in drained organic soils. Soil Biol. Biochem. 115, 178–186. https://doi.org/10.1016/j.soilbio.2017.08.025.
Lewicka-Szczebak, D., Augustin, J., Giesemann, A., Well, R., 2017. Quantifying N_2O reduction to N_2 based on N_2O isotopocules-validation with independent methods (helium incubation and ^{15}N gas flux method). Biogeosciences 14 (3), 711–732. https://doi.org/10.5194/bg-14-711-2017.
Li, Z., Gao, P., You, Y., 2018. Characterizing Hydrological Connectivity of Artificial Ditches in Zoige Peatlands of Qinghai-Tibet Plateau. Water 10 (10), 1364. https://doi.org/10.3390/w10101364.
Li, M., Shimizu, M., Hatano, R., 2015. Evaluation of N_2O and CO_2 hot moments in managed grassland and cornfield, southern Hokkaido, Japan. Catena 133, 1–13. https://doi.org/10.1016/j.catena.2015.04.014.
Lin, F., Zuo, H., Ma, X., Ma, L., 2022. Comprehensive assessment of nitrous oxide emissions and mitigation potentials across European peatlands. Environ. Pollut. 301, 119041 https://doi.org/10.1016/j.envpol.2022.119041.
Lindsay, E.A., Colloff, M.J., Gibb, N.L., Wakelin, S.A., 2010. The Abundance of Microbial Functional Genes in Grassy Woodlands Is Influenced More by Soil Nutrient Enrichment than by Recent Weed Invasion or Livestock Exclusion. Appl. Environ. Microbiol. 76 (16), 5547–5555. https://doi.org/10.1128/AEM.03054-09.
Liu, L., Chen, H., Jiang, L., Hu, J., Zhan, W., He, Y., Zhu, D., Zhong, Q., Yang, G., 2018. Water table drawdown reshapes soil physicochemical characteristics in Zoige peatlands. Catena 170, 119–128. https://doi.org/10.1016/j.catena.2018.05.025.
Liu, H., Zak, D., Rezanezhad, F., Lennartz, B., 2019. Soil degradation determines release of nitrous oxide and dissolved organic carbon from peatlands. Environ. Res Lett 14 (9), 094009. https://doi.org/10.1088/1748-9326/ab3947.
Liu, H., Wrage-Mönnig, N., Lennartz, B., 2020. Rewetting strategies to reduce nitrous oxide emissions from European peatlands. Commun. Earth Environ. 1 (1), 17. https://doi.org/10.1038/s43247-020-00017-2.
Long, X., Shen, J., Wang, J., Zhang, L., Di, H., He, J., 2017. Contrasting response of two grassland soils to N addition and moisture levels: N_2O emission and functional gene abundance. J. Soils Sediments 17 (2), 384–392. https://doi.org/10.1007/s11368-016-1559-2.
Macrae, M.L., Devito, K.J., Strack, M., Waddington, J.M., 2013. Effect of water table drawdown on peatland nutrient dynamics: Implications for climate change. Biogeochemistry 112 (1), 661–676. https://doi.org/10.1007/s10533-012-9730-3.
Maljanen, M., Hytönen, J., Martikainen, P.J., 2010. Cold-season nitrous oxide dynamics in a drained boreal peatland differ depending on land-use practice. Can. J. Forest Res. 40 (3), 565–572. https://doi.org/10.1139/X10-004.
Minkkinen, K., Ojanen, P., Koskinen, M., Penttilä, T., 2020. Nitrous oxide emissions of undrained, forestry-drained, and rewetted boreal peatlands. For. Ecol. Manag. 478, 118494 https://doi.org/10.1016/j.foreco.2020.118494.
Murphy, M.T., McKinley, A., Moore, T.R., 2009. Variations in above- and below-ground vascular plant biomass and water table on a temperate ombrotrophic peatland. Botany 87 (9), 845–853. https://doi.org/10.1139/B09-052.
Nadeem, S., Dörsch, P., Bakken, L.R., 2013. Autoxidation and acetylene-accelerated oxidation of NO in a 2-phase system: Implications for the expression of denitrification in ex situ experiments. Soil Biol. Biochem. 57, 606–614. https://doi.org/10.1016/j.soilbio.2012.10.007.
Niklaus, P.A., Roux, X.L., Poly, F., Buchmann, N., Scherer-Lorenzen, M., Weigelt, A., Barnard, R.L., 2016. Plant species diversity affects soil-atmosphere fluxes of methane and nitrous oxide. Oecologia 181 (3), 919–930. https://doi.org/10.1007/s00442-016-3611-8.
Orellana, F., Verma, P., Loheide, S.P., Daly, E., 2012. Monitoring and modeling water-vegetation interactions in groundwater-dependent ecosystems. Rev. Geophys. 50, RG3003. https://doi.org/10.1029/2011RG000383.
Pärn, J., Verhoeven, J.T.A., Butterbach-Bahl, K., Dise, N.B., Ullah, S., Aasa, A., Egorov, S., Espenberg, M., Järveoja, J., Jauhiainen, J., Kasak, K., Klemedtsson, L., Kull, A., Laggoun-Défarge, F., Lapshina, E.D., Lohila, A., Lõhmus, K., Maddison, M., Mitsch, W.J., Müller, C., Niinemets, Ü., Osborne, B., Pae, T., Salm, J.O., Sgouridis, F., Sohar, K., Soosaar, K., Storey, K., Teemusk, A., Tenywa, M.M., Tournebize, J., Truu, J., Veber, G., Villa, J.A., Zaw, S.S., Mander, Ü., 2018. Nitrogen-rich organic soils under warm well-drained conditions are global nitrous oxide emission hotspots. Nat. Commun. 9 (1). https://doi.org/10.1038/s41467-018-03540-1. https://doi.org/10.1038/s41467-018-03540-1.
Petrescu, A.M.R., Lohila, A., Tuovinen, J.P., Baldocchi, D.D., Desai, A.R., Roulet, N.T., Vesala, T., Dolman, A.J., Oechel, W.C., Marcolla, B., Friborg, T., Rinne, J., Matthes, J.H., Merbold, L., Meijide, A., Kiely, G., Sottocornola, M., Sachs, T., Zona, D., Varlagin, A., Lai, D.Y.F., Veenendaal, E., Parmentier, F.J.W., Skiba, U., Lund, M., Hensen, A., van Huissteden, J., Flanagan, L.B., Shurpali, N.J., Grünwald, T., Humphreys, E.R., Jackowicz-Korczynski, M., Aurela, M.A., Laurila, T., Grüning, C., Corradi, C.A.R., Schrier-Uijl, A.P., Christensen, T.R., Tamstorf, M.P., Mastepanov, M., Martikainen, P.J., Verma, S.B., Bernhofer, C., Cescatti, A., 2015. The uncertain climate footprint of wetlands under human pressure. Proc. Natl. Acad. Sci. 112 (15), 4594–4599. https://doi.org/10.1073/pnas.1416267112.
Qiao, M., Xiao, J., Yin, H., Pu, X., Yue, B., Liu, Q., 2014. Analysis of the phenolic compounds in root exudates produced by a subalpine coniferous species as responses to experimental warming and nitrogen fertilisation. Chem. Ecol. 30 (6), 555–565. https://doi.org/10.1080/02757540.2013.868891.
Ramirez, K.S., Craine, J.M., Fierer, N., 2010. Nitrogen fertilization inhibits soil microbial respiration regardless of the form of nitrogen applied. Soil Biology and Biochemistry 42, 2336–2338.
Ravishankara, A.R., Daniel, J.S., Portmann, R.W., 2009. Nitrous Oxide (N_2O): The Dominant Ozone-Depleting Substance Emitted in the 21st Century. Science 326 (5949), 123–125. https://doi.org/10.1126/science.1176985.
Regina, K., Silvola, J., Martikainen, P.J., 1998. Mechanisms of N_2O and NO production in the soil profile of a drained and forested peatland, as studied with acetylene, nitrapyrin and dimethyl ether. Biol. Fert. Soils 27 (2), 205–210. https://doi.org/10.1007/s003740050421.
Rinnan, R., Michelsen, A., BÅÅTh, E., Jonasson, S., 2007. Fifteen Years of Climate Change Manipulations Alter Soil Microbial Communities in a Subarctic Heath Ecosystem. Global Change Biol. 13 (1), 28–39. https://doi.org/10.1111/j.1365-2486.2006.01263.x.
Rousset, C., Clough, T.J., Grace, P.R., Rowlings, D.W., Scheer, C., 2020. Soil type, bulk density and drainage effects on relative gas diffusivity and N_2O emissions. Soil Res 58 (8), 726–736. https://doi.org/10.1071/SR20161.
Salm, J.O., Maddison, M., Tammik, S., Soosaar, K., Truu, J., Mander, Ü., 2012. Emissions of CO_2, CH_4 and N_2O from undisturbed, drained and mined peatlands in Estonia. Hydrobiologia 692 (1), 41–55. https://doi.org/10.1007/s10750-011-0934-7.
Senbayram, M., Well, R., Bol, R., Chadwick, D.R., Jones, D.L., Wu, D., 2018. Interaction of straw amendment and soil NO_3^- content controls fungal denitrification and denitrification product stoichiometry in a sandy soil. Soil Biol. Biochem. 126, 204–212. https://doi.org/10.1016/j.soilbio.2018.09.005.
Senbayram, M., Budai, A., Bol, R., Chadwick, D., Marton, L., Gündogan, R., Wu, D., 2019. Soil NO_3^- level and O_2 availability are key factors in controlling N_2O reduction to N_2 following long-term liming of an acidic sandy soil. Soil Biol. Biochem. 132, 165–173. https://doi.org/10.1016/j.soilbio.2019.02.009.
Song, X., Wei, H., Rees, R.M., Ju, X., 2022. Soil oxygen depletion and corresponding nitrous oxide production at hot moments in an agricultural soil. Environ. Pollut. 292, 118345 https://doi.org/10.1016/j.envpol.2021.118345.
Strack, M., Waddington, J.M., Bourbonniere, R.A., Buckton, E.L., Shaw, K., Whittington, P., Price, J.S., 2008. Effect of water table drawdown on peatland dissolved organic carbon export and dynamics. Hydrol. Process. 22 (17), 3373–3385. https://doi.org/10.1016/j.envpol.2021.118345.
Sun, H., Zhang, C., Song, C., Chang, S.X., Gu, B., Chen, Z., Peng, C., Chang, J., Ge, Y., 2013. The effects of plant diversity on nitrous oxide emissions in hydroponic microcosms. Atmos. Environ. 77, 544–547. https://doi.org/10.1016/j.atmosenv.2013.05.058.
Sutka, R.L., Ostrom, N.E., Ostrom, P.H., Breznak, J.A., Gandhi, H., Pitt, A.J., Li, F., 2006. Distinguishing Nitrous Oxide Production from Nitrification and Denitrification on the Basis of Isotopomer Abundances. Appl. Environ. Microbiol. 72 (1), 638–644. https://doi.org/10.1128/AEM.72.1.638-644.2006.
Tang, Y., Yu, G., Zhang, X., Wang, Q., Tian, D., Tian, J., Niu, S., Ge, J., 2019. Environmental variables better explain changes in potential nitrification and denitrification activities than microbial properties in fertilized forest soils. Sci. Total Environ. 647, 653–662. https://doi.org/10.1016/j.scitotenv.2018.07.437.

Toyoda, S., Yoshida, N., Koba, K., 2017. Isotopocule analysis of biologically produced nitrous oxide in various environments. Mass Spectrom. Rev. 36 (2), 135–160. https://doi.org/10.1002/mas.21459.

Urbanová, Z., Bárta, J., 2016. Effects of long-term drainage on microbial community composition vary between peatland types. Soil Biol. Biochem. 92, 16–26. https://doi.org/10.1016/j.soilbio.2015.09.017.

van Groenigen, J.W., Kuikman, P.J., de Groot, W.J.M., Velthof, G.L., 2005. Nitrous oxide emission from urine-treated soil as influenced by urine composition and soil physical conditions. Soil Biol. Biochem. 37 (3), 463–473. https://doi.org/10.1016/j.soilbio.2004.08.009.

Wang, D., Li, Z., Li, Z., Ma, W., Nie, X., 2019. Response of organic carbon in drainage ditch water to rainfall events in Zoige Basin in the Qinghai-Tibet Plateau. J. Hydrol. 579, 124187 https://doi.org/10.1016/j.jhydrol.2019.124187.

Wang, H., Yu, L., Zhang, Z., Liu, W., Chen, L., Cao, G., Yue, H., Zhou, J., Yang, Y., Tang, Y., He, J., 2017. Molecular mechanisms of water table lowering and nitrogen deposition in affecting greenhouse gas emissions from a Tibetan alpine wetland. Glob. Change Biol. 23 (2), 815–829. https://doi.org/10.1111/gcb.13467.

Wei, X., Cao, R., Wu, X., Eisenhauer, N., Sun, S., 2018. Effect of water table decline on the abundances of soil mites, springtails, and nematodes in the Zoige peatland of eastern Tibetan Plateau. Appl. Soil Ecol. 129, 77–83. https://doi.org/10.1016/j.apsoil.2018.05.006.

Wertz, S., Dandie, C.D., Goyer, C., Trevors, J.T., Patten, C.L., 2009. Diversity of *nirK* Denitrifying Genes and Transcripts in an Agricultural Soil. Appl. Environ. Microbiol. 75 (23), 7365–7377. https://doi.org/10.1128/AEM.01588-09.

Wilson, R.M., Hopple, A.M., Tfaily, M.M., Sebestyen, S.D., Schadt, C.W., Pfeifer-Meister, L., Medvedeff, C., McFarlane, K.J., Kostka, J.E., Kolton, M., Kolka, R.K., Kluber, L.A., Keller, J.K., Guilderson, T.P., Griffiths, N.A., Chanton, J.P., Bridgham, S.D., Hanson, P.J., 2016. Stability of Peatland Carbon to Rising Temperatures. Nat. Commun. 7 (1), 13723. https://doi.org/10.1038/ncomms13723.

Wu, X., Cao, R., Wei, X., Xi, X., Shi, P., Eisenhauer, N., Sun, S., 2017b. Soil drainage facilitates earthworm invasion and subsequent carbon loss from peatland soil. J. Appl. Ecol. 54 (5), 1291–1300. https://doi.org/10.1111/1365-2664.12894.

Wu, D., Cárdenas, L.M., Calvet, S., Brüggemann, N., Loick, N., Liu, S., Bol, R., 2017a. The effect of nitrification inhibitor on N_2O, NO and N_2 emissions under different soil moisture levels in a permanent grassland soil. Soil Biol. Biochem. 113, 153–160. https://doi.org/10.1016/j.soilbio.2017.06.007.

Wu, D., Well, R., Cárdenas, L.M., Fuß, R., Lewicka-Szczebak, D., Köster, J.R., Brüggemann, N., Bol, R., 2019. Quantifying N_2O reduction to N_2 during denitrification in soils via isotopic mapping approach: Model evaluation and uncertainty analysis. Environ. Res. 179, 108806 https://doi.org/10.1016/j.envres.2019.108806.

Wu, D., Senbayram, M., Moradi, G., Mörchen, R., Knief, C., Klumpp, E., Jones, D.L., Well, R., Chen, R., Bol, R., 2021. Microbial potential for denitrification in the hyperarid Atacama Desert soils. Soil Biol. Biochem. 157, 108248 https://doi.org/10.1016/j.soilbio.2021.108248.

Xiang, S., Guo, R., Wu, N., Sun, S., 2009. Current status and future prospects of Zoige Marsh in Eastern Qinghai-Tibet Plateau. Ecol. Eng. 35 (4), 553–562. https://doi.org/10.1016/j.ecoleng.2008.02.016.

Xu, Z., Wang, S., Wang, Z., Dong, Y., Zhang, Y., Liu, S., Li, J., 2021. Effect of drainage on microbial enzyme activities and communities dependent on depth in peatland soil. Biogeochemistry 155 (3), 323–341. https://doi.org/10.1007/s10533-021-00828-1.

Xue, D., Chen, H., Zhan, W., Huang, X., He, Y., Zhao, C., Zhu, D., Liu, J., 2021. How do water table drawdown, duration of drainage, and warming influence greenhouse gas emissions from drained peatlands of the Zoige Plateau? Land Degrad. Dev. 32 (11), 3351–3364. https://doi.org/10.1002/ldr.4013.

Yang, P., Reijneveld, A., Lerink, P., Qin, W., Oenema, O., 2022. Within-field spatial variations in subsoil bulk density related to crop yield and potential CO_2 and N_2O emissions. Catena 213, 106156. https://doi.org/10.1016/j.catena.2022.106156.

Zeng, J., Chen, H., Bai, Y., Dong, F., Peng, C., Yan, F., Cao, Q., Yang, Z., Yang, S., Yang, G., 2021. Water table drawdown increases plant biodiversity and soil polyphenol in the Zoige Plateau. Ecol. Indic. 121, 107118 https://doi.org/10.1016/j.ecolind.2020.107118.

Zhang, H., Yao, Z., Wang, K., Zheng, X., Ma, L., Wang, R., Liu, C., Zhang, W., Zhu, B., Tang, X., Hu, Z., Han, S., 2018. Annual N_2O emissions from conventionally grazed typical alpine grass meadows in the eastern Qinghai-Tibetan Plateau. Sci. Total Environ. 625, 885–899. https://doi.org/10.1016/j.scitotenv.2017.12.216.